

Precision electroweak physics at the LHeC and FCC-eh

Daniel Britzger*

Physikalisches Institut, Universität Heidelberg, Germany

E-mail: britzger@physi.uni-heidelberg.de

Max Klein

Physics Department, University of Liverpool, UK

E-mail: mklein@hep.ph.liv.ac.uk

Electroweak (EW) physics at the future electron-proton colliders LHeC and FCC-eh is studied. Simulated neutral-current and charged-current deep-inelastic scattering cross sections are employed for simultaneous determinations of the parton distribution functions of the proton together with the fundamental parameters of the EW theory, including their statistical and systematic uncertainties. Uncertainties of the W and Z boson masses are determined and compared to uncertainties obtained from HERA combined data. The LHeC data will allow for a determination of m_W with an uncertainty of 17 MeV, and the FCC-eh with 10 MeV, thus exceeding the precision of the currently most precise single measurements. The LHeC or FCC-eh data will allow for a precision determination of the vector and axial-vector couplings of the light quarks to the Z -boson, with uncertainties being smaller by an order of magnitude than current measurements. It is shown, that the measurements of the EW parameters are not limited by the precision of the parton distribution functions, which have also to be determined from the same data. The measurements of the inclusive DIS cross sections as a function of the four-momentum transfer squared Q^2 will allow for high precision tests of the scale dependence of the EW theory in the range from a few GeV up to the TeV regime from a single process.

XXV International Workshop on Deep Inelastic Scattering and Related Topics

3-7 April, 2017

University of Birmingham, UK

*Speaker.

1. Introduction

Electron-proton collisions have been extensively studied by the H1 and ZEUS experiments at the HERA collider at center-of-mass energies of $\sqrt{s} = 318 \text{ GeV}$. The LHeC [1] and FCC-eh are future proposed electron-proton colliders at CERN, with \sqrt{s} of 1.3 TeV or 3.5 TeV, respectively, thus exceeding significantly the previously studied kinematic region. Both facilities foresee the use of a longitudinally polarised electron beam with energy $E_e = 60 \text{ GeV}$, which is collided with either protons from the LHC ($E_p = 7 \text{ TeV}$) or the FCC-pp ($E_p = 50 \text{ TeV}$). The large \sqrt{s} and hugely increased integrated luminosities of up to ab^{-1} as compared to HERA will allow for precise measurements of the inclusive neutral-current and charged-current deep-inelastic scattering cross sections (NC and CC DIS) at virtualities $Q^2 \gtrsim m_{W/Z}^2$ where electroweak (EW) effects are important. This article presents studies of EW effects in inclusive NC and CC DIS at the LHeC and FCC-eh. The sensitivity of inclusive DIS cross sections on fundamental EW parameters, such as the W and Z -boson masses (m_W and m_Z) or the weak neutral couplings of the light quarks ($v_{u,d}$ and $a_{u,d}$), are studied.

2. Electroweak effects in NC and CC DIS

NC interactions in the process $e^\pm p \rightarrow e^\pm X$ are mediated by virtual photons (γ) or Z bosons in the t -channel. CC interactions, having a neutrino in the final state, are mediated by W -bosons. The predictions for inclusive NC and CC DIS cross sections are expressed in terms of generalised structure functions. For NC DIS they are \tilde{F}_2^\pm , $x\tilde{F}_3^\pm$ and \tilde{F}_L^\pm and the cross section is determined as

$$\frac{d^2\sigma^{\text{NC}}(e^\pm p)}{dx dQ^2} = \frac{2\pi\alpha^2}{xQ^2} \left[Y_+ \tilde{F}_2^\pm(x, Q^2) \mp Y_- x\tilde{F}_3^\pm(x, Q^2) - y^2 \tilde{F}_L^\pm(x, Q^2) \right], \quad (2.1)$$

with α being the fine structure constant. The helicity dependence of the interactions is contained in the terms $Y_\mp = 1 \pm (1-y)^2$ with y being the inelasticity of the process, and x is defined as $x = Q^2/(ys)$. The contributions from F_L are only sizeable at high y and thus not discussed in the following. The generalised structure functions are further decomposed into contributions from pure photon-exchange, pure Z -exchange and γZ -interference and read

$$\tilde{F}_2^\pm = F_2 - (v_e \pm P_e a_e) \kappa_Z F_2^{\gamma Z} + \left[(v_e^2 + a_e^2) \pm 2P_e a_e \right] \kappa_Z^2 F_2^Z \quad (2.2)$$

$$x\tilde{F}_3^\pm = -(a_e \pm P_e v_e) \kappa_Z F_3^{\gamma Z} + \left[2v_e a_e \pm P_e (v_e^2 + a_e^2) \right] \kappa_Z^2 F_3^Z, \quad (2.3)$$

with P_e denoting the longitudinal polarisation of the electron beam and using for the normalisation κ_Z and the Fermi coupling constant (G_F)

$$\kappa_Z(Q^2) = \frac{Q^2}{Q^2 + m_Z^2} \frac{G_F m_Z^2}{2\sqrt{2}\pi\alpha} \quad \text{and} \quad G_F = \frac{2\pi\alpha}{2\sqrt{2}m_W^2} \left(1 - \frac{m_W^2}{m_Z^2} \right)^{-1} (1 + \Delta r). \quad (2.4)$$

The term $\Delta r = \Delta r(\alpha, m_W, m_Z, m_t, m_H, \dots)$ contains corrections to the muon decay and its calculation takes α and the boson and fermion masses as input [2]. The structure functions are related to linear combinations of the quark and anti-quark momentum distributions, xq and $x\bar{q}$, and read in

the quark-parton model

$$\left[F_2, F_2^{\gamma Z}, F_2^Z \right] = x \sum_q \left[e_q^2, 2e_q v_q, v_q^2 + a_q^2 \right] \{q + \bar{q}\}, \quad (2.5)$$

$$\left[F_3^{\gamma Z}, F_3^Z \right] = x \sum_q \left[2e_q a_q, 2v_q a_q \right] \{q + \bar{q}\}, \quad (2.6)$$

where a_q and v_q are the weak neutral vector and axial-vector couplings of the quarks to the Z-boson. The couplings are predicted by the Standard Model (SM) to be $a_q = I_{q,L}^{(3)}$ and $v_q = I_{q,L}^{(3)} - 2e_q \sin^2 \theta_W$, with $I_{q,L}^{(3)}$ being the third component of the left-handed isospin. In the present study these couplings may be considered as additional parameters and thus have to be determined from the simulated, experimental data.

3. Simulated NC and CC DIS data

Inclusive NC and CC DIS data are simulated for the expected LHeC and FCC-eh running conditions. The simulated data sets comprise electron and positron beams with different energies and polarisation states, and different proton beam energies. A summary of the NC and CC data and the expected integrated luminosities is provided in table 1. A high polarisation will be of particular im-

lepton type	E_e [GeV]	P_e	E_p [TeV]	\mathcal{L} [fb ⁻¹]	Cross sections
e^-	60 (60)	-0.8	50 (7)	1000	NC, CC
e^-	60 (60)	+0.8	50 (7)	300	NC, CC
e^+	60 (60)	0	50 (7)	100	NC, CC
e^-	20 (60)	0	7 (1)	100	NC, CC

Table 1: Simulated data sets for different beam parameters and their expected luminosities for FCC-eh and LHeC (in parenthesis).

portance for a precise determination of the weak neutral vector couplings of the light quarks. The assumptions made for the individual sources of the uncertainties are summarised in table 2. The

Source of uncertainty	Error on source or cross section
Scattered electron energy scale $\Delta E'_e/E'_e$	0.1 %
Scattered electron polar angle	0.1 mrad
Hadronic energy scale $\Delta E_h/E_h$	0.5 %
Calorimeter noise (only $y < 0.01$)	1 – 3 %
Radiative corrections	0.3 %
Photoproduction background (only $y > 0.5$)	1 %
Global efficiency uncertainty	0.5 %

Table 2: Assumptions imposed on the size of uncertainties for the simulated NC DIS cross sections.

size of uncertainties is typical inline with the best values achieved by H1 at HERA, and thus may be considered to be conservative as advanced detector concepts and hugely increased luminosities should yield significantly reduced uncertainties.

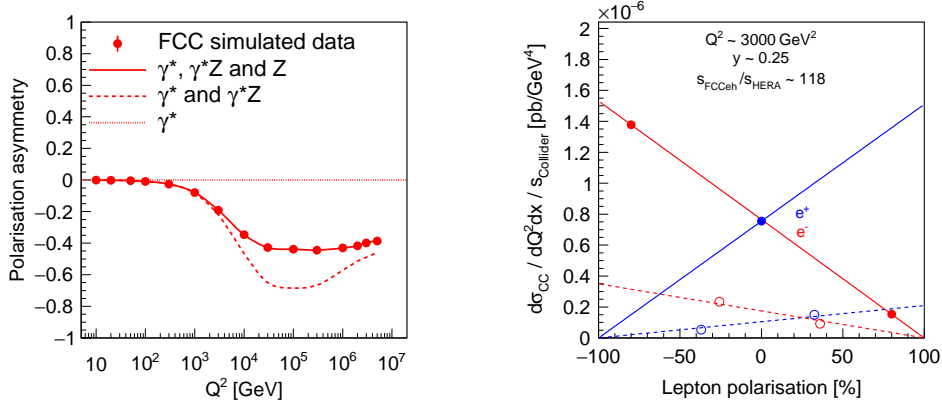


Figure 1: Left: Neutral-current polarisation asymmetry as a function of Q^2 integrated over x for FCC-eh simulated data. The polarisation asymmetry is displayed for pure photon exchange, which is zero by definition, for calculations including only the interference terms γ^*Z , and for predictions including also purely weak effects, ZZ . The full circles illustrate simulated data points, which have uncertainties invisible at the chosen scales. Right: Charged-current cross sections measured with different lepton polarisation states and for electron (red) and positron (blue) beams. The full circles illustrate FCC-eh simulated data, whereas the open circles show H1 measurements. The data are scaled by the center-of-mass energies of the respective collider. The error bars are smaller than the markers.

The size of electroweak contributions to the NC DIS cross sections may be expressed by the polarisation asymmetry, defined as

$$A = \frac{2}{P_L - P_R} \frac{\sigma(P_L) - \sigma(P_R)}{\sigma(P_L) + \sigma(P_R)}, \quad (3.1)$$

using the cross sections measured for two distinct beam polarisations P_L and P_R . Its dependence as a function of Q^2 for simulated FCC-eh data is displayed in figure 1 (left), where calculations involving exclusively γ -exchange, or γ and γZ -exchange are displayed in addition. The future FCC-eh data will grossly extend measurements by HERA, which did not exceed $Q^2 \gtrsim 10^4 \text{ GeV}^2$, to the regions where contributions from purely Z -exchange are relevant.

The simulated CC DIS cross sections for the different beam conditions at a given value of Q^2 and y are compared to data by H1 in figure 1 (right). At the displayed value of $Q^2 = 3000 \text{ GeV}^2$, the FCC-eh cross sections will be much higher than at HERA. At the selected Q^2 value, helicity effects of CC cross sections are irrelevant for FCC-eh and thus e^+ and e^- cross sections are of the same size for unpolarised beams because they are at low- x and thus mainly gluon initiated.

4. Determination of EW parameters

4.1 Methodology of a combined EW and QCD fit

The simulated NC and CC DIS data are employed for a determination of the parameters of the EW theory. EW parameters are determined in a simultaneous fit together with parameters of the parton distribution functions of the proton (PDFs), denoted as ‘PDF+EW-fit’. This is because the

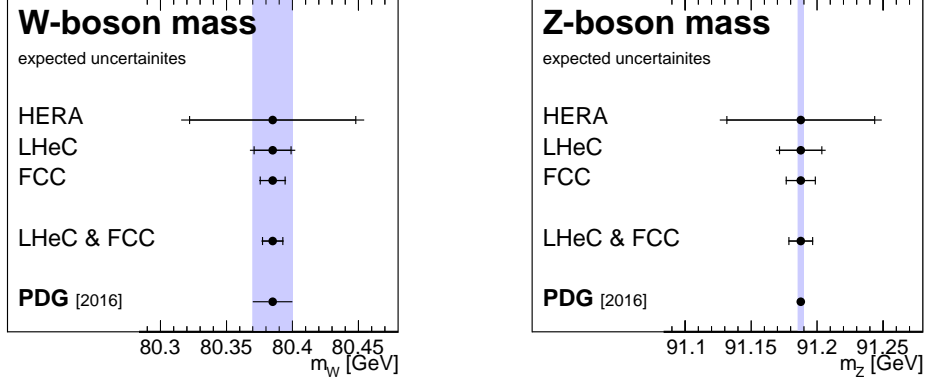


Figure 2: Measurements of the W -boson mass (left) and Z -boson mass (right) from HERA, LHeC and FCC-eh (simulated) data and compared to the PDG values.

PDFs have to be determined from the same data, and by performing a simultaneous determination of the PDFs and EW parameters the uncertainties of the PDFs are accounted for accordingly. The fitting methodology follows closely previous approaches [3, 4, 5] and it is observed that the prospects for the EW parameters are insensitive to details of the PDF fit methodology. The calculations are performed in the on-shell scheme, where the theory is expressed in terms of α , m_W , m_Z , and Δr .

4.2 W-boson, Z-boson and top-quark masses

The uncertainty values of m_W and m_Z are determined in the PDF+EW-fit, where one of the masses is determined together with the PDFs, while the other boson mass is taken as external input. The expected uncertainties are displayed in figure 2 and compared to the PDG values [6], and to the uncertainties obtained when performing our PDF+EW-fit to the final combined HERA data [3]. The expected uncertainties of m_W are

$$\begin{aligned}\Delta m_W(\text{LHeC}) &= \pm 14_{(\text{exp})} \pm 10_{(\text{PDF})} \text{ MeV} \quad \text{and} \\ \Delta m_W(\text{FCC-eh}) &= \pm 9_{(\text{exp})} \pm 4_{(\text{PDF})} \text{ MeV},\end{aligned}$$

for LHeC and FCC-eh, respectively, where the breakdown into experimental and PDF uncertainties is obtained by repeating the fit with PDF parameters fixed. The expected uncertainties of m_Z are about 19 MeV and 11 MeV for LHeC and FCC-eh, respectively, and are thus of similar size than those of m_W . The expected precision of m_Z can not compete with the precise measurements at the Z -pole by the LEP and SLC experiments, but the future ep facilities will test the SM much more precisely than hitherto, and they will improve significantly the current precision of m_W .

A simultaneous determination of m_W and m_Z together with the PDFs is performed and results are compared to a determination from H1 [5] in figure 3 (left). Due to the large correlation between m_W and m_Z , HERA data is not sufficient to determine those values reliably. Contrarily, the highly increased center-of-mass energy of LHeC or FCC-eh will allow for such a simultaneous determination of m_W and m_Z with high precision.

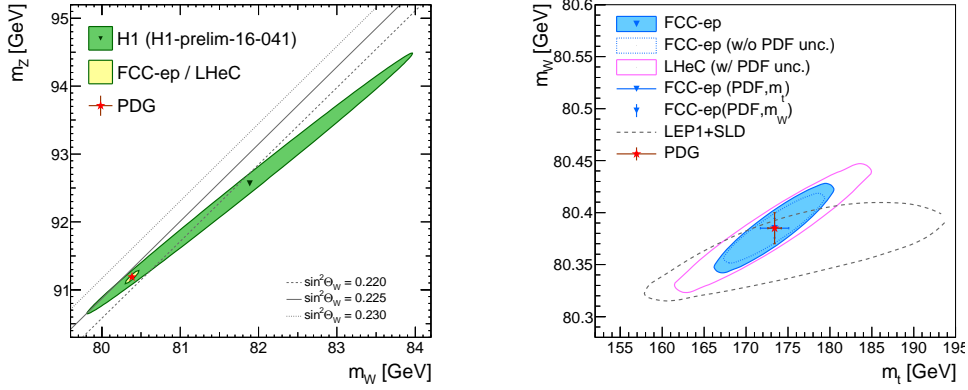


Figure 3: Simultaneous determination of m_W and m_Z from simulated LHeC and FCC-eh data in comparison to a determination by H1 (left). The thin lines illustrate the corresponding value of $\sin^2 \theta_W$ in the on-shell scheme. Simultaneous determination of m_W and m_t from simulated LHeC and FCC-eh data (left) in comparison to the achieved precision by the LEP+SLD combination.

The top-quark mass m_t contributes to the calculations through Δr . A simultaneous determination of m_W and m_t , where m_Z is an external input, is presented in figure 3 (right) and compared to results from LEP+SLD [7]. Both, the LHeC and FCC-eh, will be able to improve the combined results from the LEP and SLC experiments, and thus provide a very sensitive test of the EW sector of the SM. The indirect constraints from inclusive DIS LHeC (FCC-eh) data will allow to determine m_t with an uncertainty of 1.8 GeV (1.5 GeV). Additional direct measurements of m_t will significantly improve these results.

4.3 Weak neutral couplings of light quarks

The vector and axial-vector couplings of up-type and down-type quarks to the Z ($v_{u/d}$ and $a_{u/d}$) are determined in a single fit of the four couplings together with the PDFs. Resulting uncertainties are presented in table 3 and compared to the currently most precise measurements [6]. The two-

Coupling parameter	PDG	Expected uncertainties	
		LHeC	FCC-eh
a_u	$0.50^{+0.04}_{-0.05}$	0.006	0.003
a_d	$-0.514^{+0.050}_{-0.029}$	0.011	0.005
v_u	0.18 ± 0.05	0.003	0.002
v_d	$-0.35^{+0.05}_{-0.06}$	0.008	0.005

Table 3: Standard model expectations for the light-quark weak neutral couplings (a_u, a_d, v_u, v_d) together with the currently most precise uncertainties (PDG [6]) and the prospected uncertainties for LHeC and FCC-eh.

dimensional uncertainty contours ($\Delta\chi^2 = 2.3$) are displayed in figure 4 for each single quark flavor and compared to recent measurements. While the current determinations from e^+e^- , ep or $p\bar{p}$ data have all somewhat similar precision, the future ep facilities will greatly improve the precision of the weak neutral couplings and expected uncertainties are an order of magnitude smaller than the currently most precise ones [6].

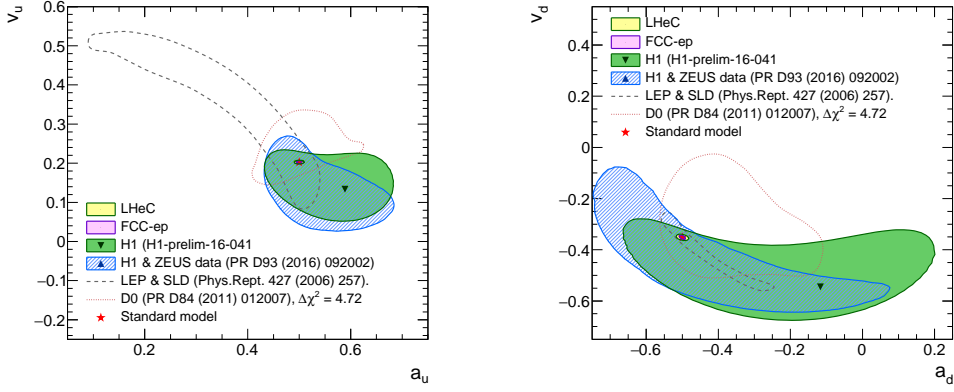


Figure 4: Results for the vector and axial-vector couplings of the up-type (left) and down-type (right) quarks to the Z at the 68 % confidence level (C.L.) for simulated LHeC and FCC-eh data. The results are compared to measurements by H1 [5] and D0 [8], and to determinations using H1 and ZEUS [9] or LEP and SLD data [7]. The standard model expectations are displayed by a red star.

4.4 Scale dependence of $\sin^2 \theta_W$

The inclusive DIS cross sections are measured over a large kinematic range. This allows for a unique test of the scale dependence of EW effects from a single process. A fit of PDF parameters together with 14 parameters representing the weak-mixing angle $\sin^2 \theta_W$ at individual Q^2 values of the simulated data is performed. The results are presented in figure 5. In the SM, no scale dependence is built in in the on-shell scheme since $\sin^2 \theta_W$ can be equivalently expressed as a determination of m_W . In this case the prospected precision would be around 10 MeV (15 MeV) over a large kinematic range for the FCC-eh (LHeC).

This study, which is to be performed in the $\overline{\text{MS}}$ scheme next, well illustrates the expected sensitivity to EW effects at the different scales in the range from 10 GeV up to the TeV regime.

5. Summary and conclusion

Simulated neutral-current and charged-current DIS data are employed for a determination of the fundamental parameter of the electroweak theory. The LHeC or FCC-eh will allow for precision measurements of the electroweak sector, by far exceeding the precision of HERA measurements and in general with comparable or even higher precision than the LEP or LHC experiments. These measurements thus provide complementary tests of the Standard Model in the domain of space-like momentum transfer. The measurements of the EW parameters are not limited by the precision

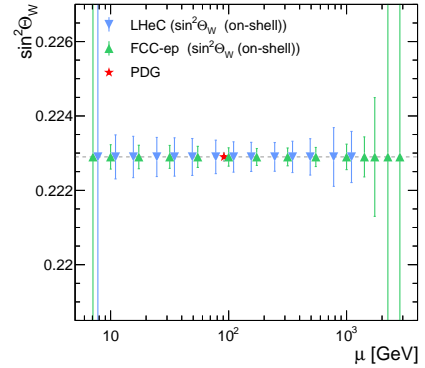


Figure 5: The weak-mixing angle $\sin^2 \theta_W$ in the on-shell scheme definition at different values of Q^2 .

of the parton distribution functions, which have also to be determined from the same data. It is demonstrated, that the LHeC or FCC-eh will allow for a very precise determination of the light-quark weak couplings. Whether with that new level of precision deviations from the SM coupling predictions may be revealed is for future ep data to tell.

References

- [1] LHeC Study group, J.L. Abelleira *et al.*, J.Phys. G39 (2012) 075001, arXiv:1206.2913.
- [2] H. Spiesberger, “EPRC. A program package for electroweak physics at HERA,” in proceedings of the 95-96 Workshop on Future Physics at HERA, part 2. 1995.
- [3] H1 and ZEUS Collaboration, H. Abramowicz *et al.*, Eur. Phys. J. C75 (2015) 580, arXiv:1506.06042.
- [4] M. Klein and V. Radescu, “Partons from the LHeC,” CERN-LHeC-Note-2013-002, Jul 2013, <https://cds.cern.ch/record/1564929>.
- [5] H1 Collaboration, H1-prelim-16-041, 2016, available online.
- [6] Particle Data Group Collaboration, C. Patrignani *et al.*, Chin. Phys. C40 (2016) 100001.
- [7] ALEPH, DELPHI, L3, OPAL and SLD Collaborations, S. Schael *et al.*, Phys. Rept. 427 (2006) 257, hep-ex/0509008.
- [8] D0 Collaboration, V.M. Abazov *et al.*, Phys.Rev. D84 (2011) 012007, arXiv:1104.4590.
- [9] ZEUS Collaboration, H. Abramowicz *et al.*, Phys.Rev. D93 (2016) 092002.